ACS Macro Letters

Letter

pubs.acs.org/macroletters

In Situ Deposition of PLGA Nanofibers via Solution Blow Spinning

Adam M. Behrens,[†] Brendan J. Casey,[‡] Michael J. Sikorski,[†] Kyle L. Wu,[§] Wojtek Tutak,[∥] Anthony D. Sandler,[§] and Peter Kofinas*[,†]

[†]Fischell Department of Bioengineering, University of Maryland, 2330 Jeong H. Kim Engineering Building, College Park, Maryland, United States

[‡]Office of Medical Products and Tobacco, Center for Devices and Radiological Health, Office of Science and Engineering Laboratories, Division of Chemistry and Materials Science, U.S. Food and Drug Administration, 10903 New Hampshire Ave, Silver Spring, Maryland, United States

[§]Sheikh Zayed Institute for Pediatric Surgical Innovation at Children's National Medical Center, 111 Michigan Ave NW, Washington, District of Columbia, United States

[∥]American Dental Association Foundation, National Institute of Standards and Technology, 100 Bureau Drive, Building 224, Room A153, Gaithersburg, Maryland, United States

Supporting Information

ABSTRACT: Nanofiber mats and scaffolds have been widely investigated for biomedical applications. Commonly fabricated using electrospinning, nanofibers are generated ex situ using an apparatus that requires high voltages and an electrically conductive target. We report the use of solution blow spinning to generate conformal nanofiber mats/meshes on any surface in situ, utilizing only a commercial airbrush and compressed CO_2. Solution and deposition conditions of PLGA nanofibers were optimized and mechanical properties characterized with dynamic mechanical analysis. Nanofiber mat degradation was monitored for morphologic and molecular weight changes in vitro. Biocompatibility of the direct deposition of nanofibers onto two cell lines was demonstrated in vitro and interaction with blood was qualitatively assessed with scanning electron microscopy. A pilot animal study illustrated the wide potential of this technique across multiple surgical applications, including its use as a surgical sealant, hemostatic, and buttress for tissue repair.

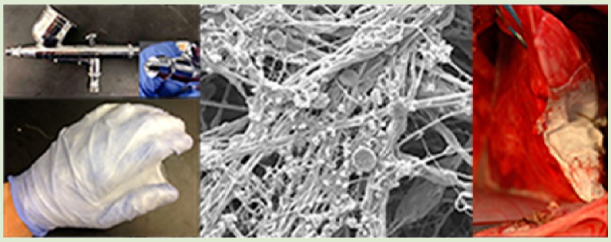

Nanofiber mats and scaffolds have a wide range of biomedical applications including drug delivery,[1] wound dressings,[2] tissue engineering,[3] and enzyme immobilization.[4] Nanofibers are often generated by electrospinning, a process that utilizes an electric field applied to a drop of polymer melt or solution on the tip of a nozzle.[5] The droplet deforms forming a Taylor cone, and a charged jet accelerates toward the target, generating nanofibers.[6] While electrospinning is a powerful and widely studied technique, it requires specialized equipment, high voltages, and electrically conductive targets. It also suffers from a relatively low deposition rate. These restrictions prohibit the use of electrospinning for any in situ deposition of fibers in surgery or for conformal coverage of nonconductive targets without the use of polymer melts[7] or the assistance of air flow.[8]

Solution blow spinning is a promising alternative that requires a simple apparatus, a concentrated polymer solution in a volatile solvent, and a high-pressure gas source.[9] Commercial airbrushes, typically used for painting, have successfully generated nanofibers through this technique.[10,11] Many polymer/solvent systems and deposition conditions have been investigated, but convincing control over fiber diameter has not been demonstrated.[12−16]

Applications that are pursued are largely analogous to electrospinning and include enzyme immobilization,[17] drug delivery,[18] and microfiltration.[19] The reported examples of this technique cite the ease of use and rapid deposition rate as compared to electrospinning.[9,11,12] Tutak et al. were the first to move toward using the method to generate conformal coatings for tissue engineering scaffolds, but no exploration into in situ deposition has yet been reported.[11]

The possibility of direct deposition introduces a host of new applications and advantages over preformed nanofiber mats/meshes and scaffolds. On-demand fabrication of conformal nanofiber mats/meshes allows for precise and site-specific construction. This could be exceedingly useful for reconstruction of tissue defects such as hernias, which treatment frequently uses preformed polymer mats with a high incidence of recurrent herniation and bowel obstruction.[20] The approach also holds great promise as a surgical sealant in place of or in addition to sutures in applications such as vascular, intestinal, or airway anastomosis. These procedures can be technically difficult and, when complications of leakage occur, have high

Received: January 27, 2014
Accepted: February 24, 2014
Published: February 26, 2014

   dx.doi.org/10.1021/mz500049x | *ACS Macro Lett.* 2014, 3, 249−254

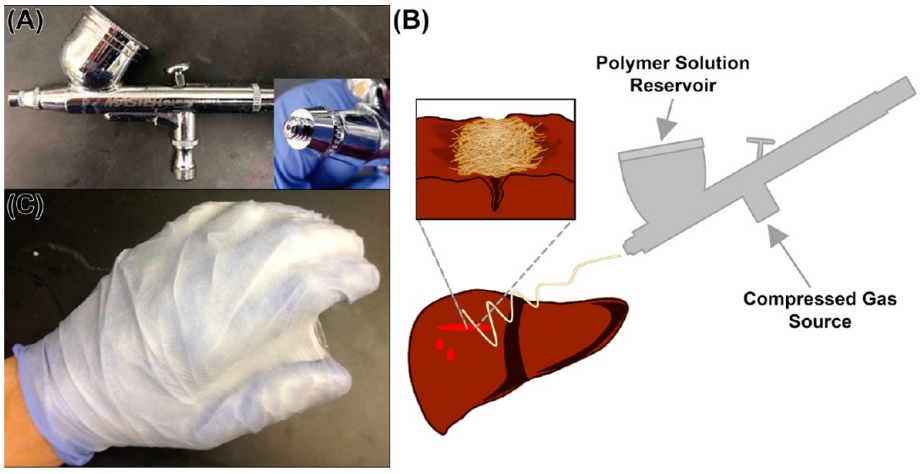

Figure 1. (A) Commercial airbrush used for nanofiber deposition. (B) Schematic representation of solution blow spinning procedure being applied to a liver injury. (C) Conformal nanofiber coating on a gloved hand.

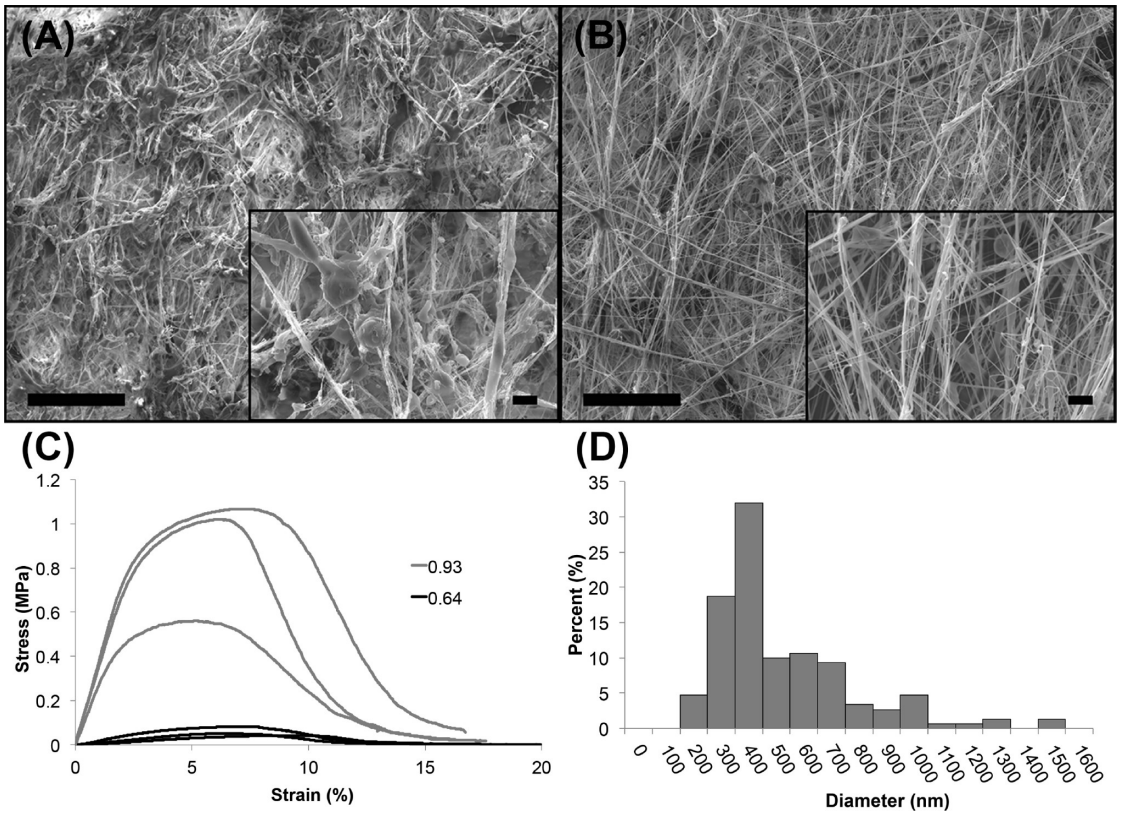

Figure 2. (A, B) Scanning electron microscopy (SEM) micrographs of blow spun 10% PLGA in acetone. (A) Solution of 0.64 IV PLGA, at a CO_2 flow rate of 13 SCFH. (B) Solution of 0.93 IV PLGA at a CO_2 flow rate of 13 SCFH. Scale bars for (A, B) are 100 and 10 μm in the inset. (C) Stress strain curves of 0.93 IV PLGA and 0.64 IV PLGA nanofiber mats (n = 3). (D) Size distribution of nanofiber diameter for optimal solution and deposition conditions (n = 150).

morbidity.[21,22] Solution blow spinning could also be useful in areas requiring the use of a hemostatic material or sealant, especially when large areas are exposed and conventional suturing may not be possible, as is the case with liver and lung resections.[23−25]

Here we use solution blow spinning to fabricate conformal mats of poly(lactic-*co*-glycolic acid) (PLGA) in situ using a commercial airbrush and compressed CO_2 (Figure 1a,b). This technique allows for rapid conformal nanofiber deposition onto any substrate (Figure 1c). Solutions composed of 10% (w/v) PLGA of two different inherent viscosities, corresponding to higher and lower molecular weights, were investigated (0.93 IV and 0.64 IV PLGA) in acetone at three different gas flow rates (Figure 2a,b and S1). Having analogous constraints to electrospinning, solution concentration, polymer molecular weight, solvent, and specific deposition conditions are required for nanofiber generation. The key parameter for the resulting morphology of solution blow spinning is the concentration (c) with respect to polymer chain entanglement, specifically the overlap concentration (c^*).[10] Solutions with $c > c^*$ form fibers,

dx.doi.org/10.1021/mz500049x | *ACS Macro Lett.* 2014, 3, 249−254

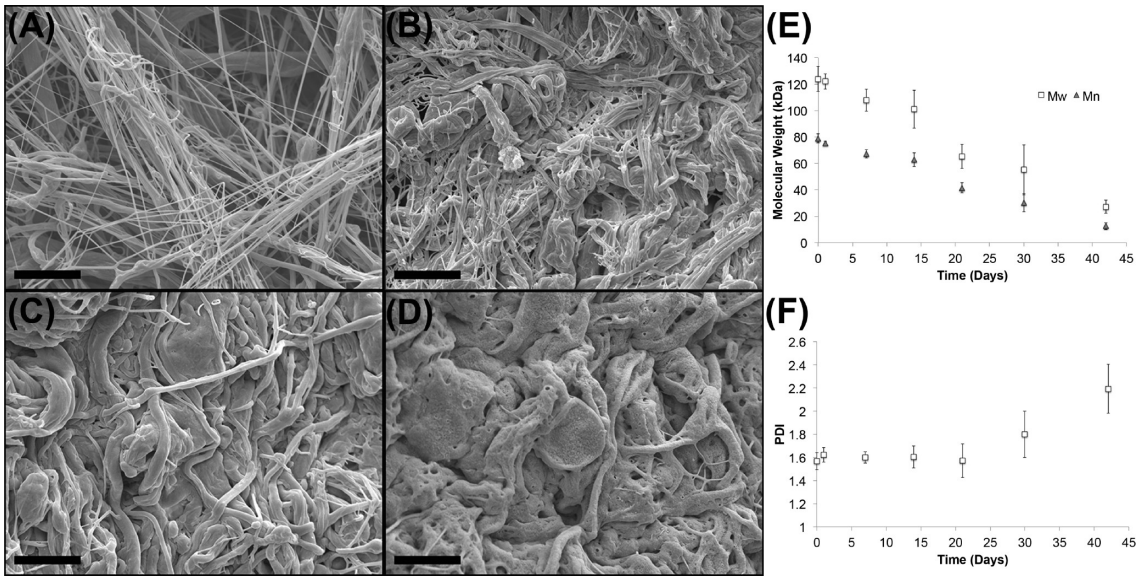

Figure 3. SEM of PLGA nanofiber degradation at 0 (A), 7 (B), 14 (C), and 42 (D) days. Scale bars correspond to 20 μm. (E) PLGA molecular weight over 42 days of nanofiber degradation (n = 3). (F) PDI change over the same time scale (n = 3).

$c \sim c^*$ form beads on a string, and $c < c^*$ form a corpuscular morphology. Fiber morphology can be seen in Figure 2b and beads on a string morphology can be seen in Figure S1c. The solution and deposition conditions that resulted in rapid generation of uniform nanofibers were found to be 10% (w/v) 0.93 IV PLGA in acetone with a 13 SCFH CO_2 gas flow rate (Figure 2b).

The resulting nanofiber mat had an average nanofiber diameter of 474 ± 262 nm and a median value of 377 nm (Figure 2d). This range of nanofiber diameter is consistent with fibrin fiber diameter (~376 nm).[26] Dynamic mechanical analysis was performed to evaluate differences in mechanical properties between solution blow spun 0.93 IV and 0.64 IV PLGA (Figure 2c). The ultimate strength was determined by the maximum of the stress−strain curve and the Young's modulus by the slope between 0 and 1% strain. The 0.93 IV PLGA had an average ultimate strength of 0.88 ± 0.28 MPa and a Young's modulus of 0.33 ± 0.06 MPa. The 0.64 IV PLGA had an average ultimate strength of 0.06 ± 0.02 MPa and a Young's modulus of 0.01 ± 0.01 MPa. The mechanical properties of the 0.93 IV PLGA nanofiber mats were significantly better than the same deposition conditions using the 0.64 IV PLGA. The Young's modulus of the optimal mat (0.88 MPa) was near that of fibrin (1−10 MPa) and many human tissues (~1 MPa).[27,28] These characteristics are well suited for in vivo use as tissue mimics in a variety of applications without the complications and costs associated with biologically derived materials.

After identifying the optimal solution and deposition conditions, PLGA nanofiber degradation was evaluated over 42 days for morphologic and molecular weight changes (Figure 3). Nanofiber morphology changed noticeably over this time scale. As fibers degraded there was an increase in average diameter as a result of fibers fusing together, and a majority of the mat porosity was lost by day 7 (Figure 3b). As degradation continued (7−42 days), fibers welded into each other forming a more homogeneous structure with evidence of obvious surface pitting and pore formation on day 30 and 42 (Figures S2 and 3d). During this same time frame, weight average molecular weight (M_w) and number average molecular weight (M_n) decreased in a linear manner from day 0 at M_w = 123.9 ± 9.4 kDa and M_n = 78.9 ± 3.4 kDa to day 42 at M_w = 27.2 ± 5.1 kDa and M_n= 12.5 ± 2.6 kDa (Figure 3e). The polydispersity index (PDI) increased from 1.6 ± 0.1 to 2.2 ± 0.2 during this period (Figure 3F). This linear decrease in molecular weight over a 42 day period corresponds to a M_w decrease of ~78% and a M_n decrease of ~84%. A linear degradation profile is consistent with surface erosion in contrast to bulk erosion.[29] The high surface area/volume of the nanofibers presumably allows for quicker diffusion and neutralization of the acidic degradation species that typically cause autocatalytic degradation in bulk erosion. This degradation profile can be altered by adjusting the ratio of lactic to glycolic acid in the copolymer.[30]

Biocompatibility of solution blow spinning PLGA/acetone directly onto cells was quantitatively evaluated with an MTS cell viability assay. All experimental groups (CO_2, acetone, PLGA/acetone) showed no statistical difference in cell viability as compared to the live control group for both L929 mouse fibroblasts and human coronary arterial endothelial cells (p < 0.05, Figure 4). Qualitative evaluation of blood interaction with

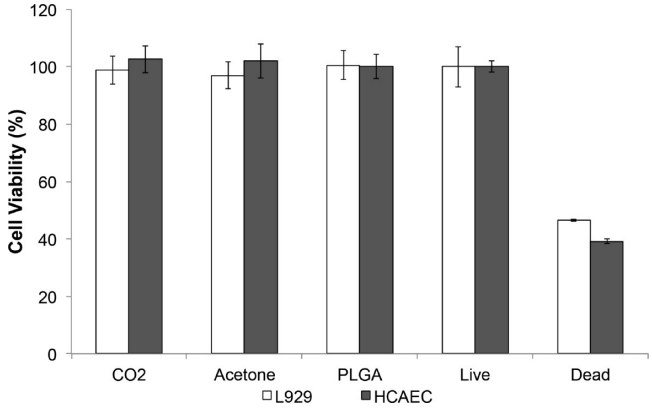

Figure 4. MTS cell viability assay of L929 mouse fibroblasts (L929) and human coronary atrial endothelial cells (HCAEC) showing no decrease in viability. Data reported as percent of live control (n = 3). Error bars reported as standard deviation.

dx.doi.org/10.1021/mz500049x | ACS Macro Lett. 2014, 3, 249−254

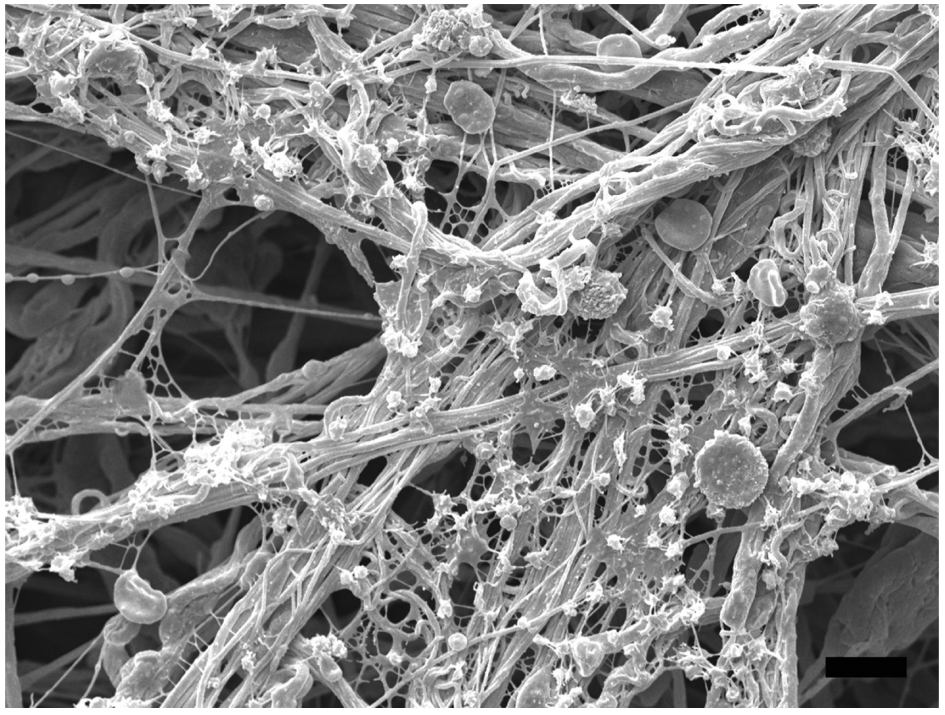

Figure 5. SEM of PLGA nanofibers incubated with citrated whole human blood. Scale bar represents 10 μm.

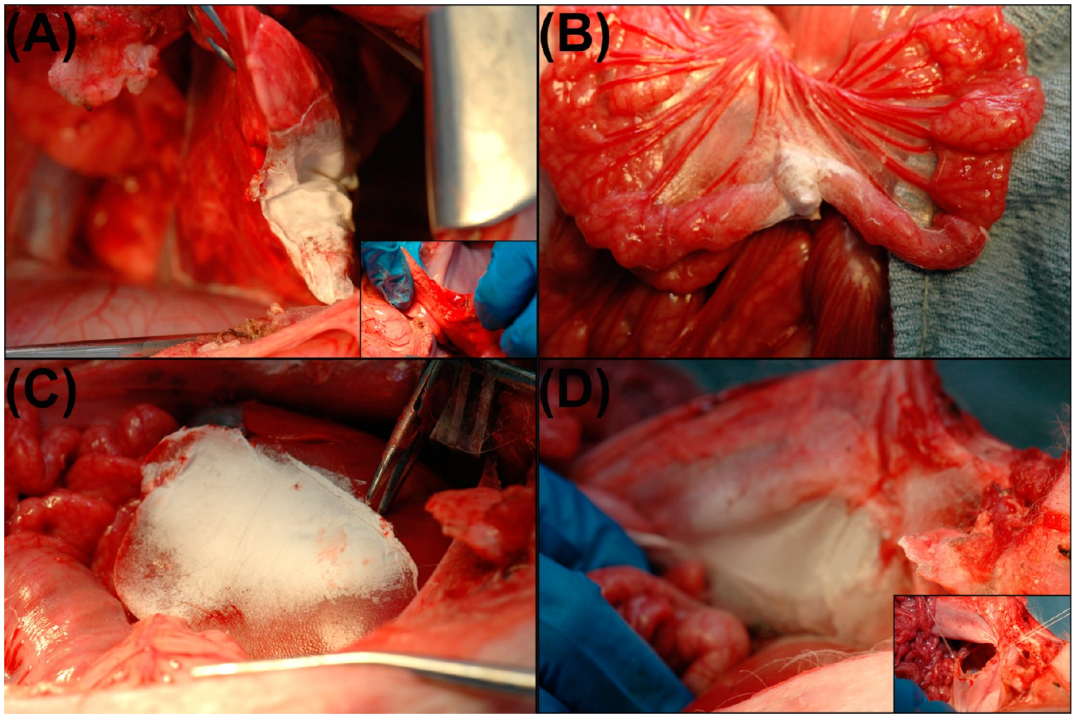

Figure 6. Direct deposition of conformal PLGA nanofiber mats: (A) Lung resection; (B) Intestinal anastomosis; (C) Liver injury; (D) Diaphragmatic hernia.

nanofiber mats was completed using SEM (Figure 5). After an hour incubation and washing with PBS there was significant platelet and erythrocyte adsorption onto the nanofiber matrix.

While solution blow spinning can be used with a variety of compressed gases, CO_2 was chosen for its potential for in situ deposition. Other compressed gases carry the risk of air embolism; CO_2 avoids this complication due to its solubility in blood.[31,32] Similarly, safety considerations must be given to the choice of polymer and solvent. Nondegradable polymers have the potential to cause harm if inhaled and most volatile solvents are too toxic to be considered for direct application. While the use of acetone may not be ideal, cell viability data from two cell lines suggests that the amount reaching the surface must be minimal (Figure 4). Additionally, for fibers to be generated and maintained, any solvent must evaporate from the system. At the highest gas flow rate tested (15 SCHF), nanofibers seemed to

dx.doi.org/10.1021/mz500049x | *ACS Macro Lett.* 2014, 3, 249−254

weld back together (Figure S1f). This can be attributed to the drop in temperature resulting from the compressed CO_2 release, leading to a decreased evaporation rate of acetone in the system. This led to the choice of the 13 SCHF flow rate for all subsequent experimentation (Figure 2b).

To demonstrate possible future applications of solution blow spinning, PLGA nanofiber mats were directly deposited in multiple surgical models in a single piglet animal model. These include lung resection, intestinal anastomosis, superficial liver injury, and diaphragmatic hernia (Figure 6). In all cases, a conformal layer of nanofibers formed over the defect in less than 1 min. Visual observation by a surgeon confirmed that PLGA nanofiber deposition stopped the liver bleeding and air leakage from the lung surface following segmentectomy. A video of PLGA nanofibers applied to the liver injury in avi format is available.

The utilization of nanofiber mats and scaffolds has been widely investigated for a variety of surgical and tissue engineering applications. The current fabrication methods, for example, electrospinning, are difficult to translate into an operating room. Solution blow spinning offers an easily adaptable alternative that has the potential to generate on-demand conformal nanofiber mats directly on a wide range of targets. The present study demonstrates facile fabrication of PLGA nanofibers using only a commercial airbrush and compressed CO_2. The solution and deposition conditions were optimized and mechanical properties characterized. Nanofiber degradation was monitored over 42 days for molecular weight and morphology changes in vitro. Biocompatibility of direct nanofiber deposition was quantitatively assessed using a cell viability assay and blood interaction assessed qualitatively with SEM. A pilot animal study was then used to demonstrate some of the possible surgical applications including use as a surgical hemostatic, a surgical sealant, and for tissue reconstruction.

■ ASSOCIATED CONTENT

Supporting Information

Experimental section and data section, including full fiber optimization and degradation SEM. A video of the application of PLGA nanofibers to the injured liver is also included. This material is available free of charge via the Internet at http://pubs.acs.org.

■ AUTHOR INFORMATION

Corresponding Author

* E-mail: kofinas@umd.edu.

Notes

The authors declare no competing financial interest.

■ ACKNOWLEDGMENTS

We would like to acknowledge the Warren Citrin Graduate Fellowship and the Sheikh Zayed Institute for Surgical Innovation for supporting this work. We would also like to thank Dr. Qijin Lu and Dr. Richard Malinauskas for their assistance with the in vitro blood protocols along with Dr. Eric Sussman for his help with the cell viability experiments. All research was performed through the University of Maryland and Children's National Medical Center. The conclusions made and items identified by brand name are the choice of the authors' and are not to be construed as conveying an official endorsement by the U.S. Food and Drug Administration.

■ REFERENCES

(1) Jing, Z.; Xu, X. Y.; Chen, X. S.; Liang, Q. Z.; Bian, X. C.; Yang, L. X.; Jing, X. B. *J. Controlled Release* **2003**, *92* (3), 227−231.
(2) Khil, M. S.; Cha, D. I.; Kim, H. Y.; Kim, I. S.; Bhattarai, N. *J. Biomed. Mater. Res. B* **2003**, *67B* (2), 675−679.
(3) Li, W. J.; Laurencin, C. T.; Caterson, E. J.; Tuan, R. S.; Ko, F. K. *J. Biomed. Mater. Res.* **2002**, *60* (4), 613−621.
(4) Wang, Z. G.; Wan, L. S.; Liu, Z. M.; Huang, X. J.; Xu, Z. K. *J. Mol. Catal., B* **2009**, *56* (4), 189−195.
(5) Agarwal, S.; Wendorff, J. H.; Greiner, A. *Polymer* **2008**, *49* (26), 5603−5621.
(6) Yarin, A. L.; Koombhongse, S.; Reneker, D. H. *J. Appl. Phys.* **2001**, *90* (9), 4836−4846.
(7) Dalton, P. D.; Klinkhammer, K.; Salber, J.; Klee, D.; Moller, M. *Biomacromolecules* **2006**, *7* (3), 686−690.
(8) Hsiao, H. Y.; Huang, C. M.; Liu, Y. Y.; Kuo, Y. C.; Chen, H. *J. Appl. Polym. Sci.* **2012**, *124* (6), 4904−4914.
(9) Medeiros, E. S.; Glenn, G. M.; Klamczynski, A. P.; Orts, W. J.; Mattoso, L. H. C. *J. Appl. Polym. Sci.* **2009**, *113* (4), 2322−2330.
(10) Srinivasan, S.; Chhatre, S. S.; Mabry, J. M.; Cohen, R. E.; McKinley, G. H. *Polymer* **2011**, *52* (14), 3209−3218.
(11) Tutak, W.; Sarkar, S.; Lin-Gibson, S.; Farooque, T. M.; Jyotsnendu, G.; Wang, D.; Kohn, J.; Bolikal, D.; Simon, C. G., Jr. *Biomaterials* **2013**, *34* (10), 2389−98.
(12) Oliveira, J. E.; Moraes, E. A.; Costa, R. G. F.; Afonso, A. S.; Mattoso, L. H. C.; Orts, W. J.; Medeiros, E. S. *J. Appl. Polym. Sci.* **2011**, *122* (5), 3396−3405.
(13) Oliveira, J. E.; Mattoso, L. H. C.; Orts, W. J.; Medeiros, E. S. *Adv. Mater. Sci. Eng.* **2013**, *2013*, 409572.
(14) Sinha-Ray, S.; Yarin, A. L.; Pourdeyhimi, B. *Carbon* **2010**, *48* (12), 3575−3578.
(15) Sinha-Ray, S.; Zhang, Y.; Yarin, A. L.; Davis, S. C.; Pourdeyhimi, B. *Biomacromolecules* **2011**, *12* (6), 2357−2363.
(16) Zhuang, X. P.; Yang, X. C.; Shi, L.; Cheng, B. W.; Guan, K. T.; Kang, W. M. *Carbohydr. Polym.* **2012**, *90* (2), 982−987.
(17) Oliveira, J. E.; Mattoso, L. H.; Medeiros, E. S.; Zucolotto, V. *Biosensors* **2012**, *2*, 70−82.
(18) Oliveira, J. E.; Medeiros, E. S.; Cardozo, L.; Voll, F.; Madureira, E. H.; Mattoso, L. H. C.; Assis, O. B. G. *Mater. Sci. Eng. C* **2013**, *33* (2), 844−849.
(19) Zhuang, X. P.; Shi, L.; Jia, K. F.; Cheng, B. W.; Kang, W. M. *J. Membr. Sci.* **2013**, *429*, 66−70.
(20) Grethel, E. J.; Cortes, R. A.; Wagner, A. J.; Clifton, M. S.; Lee, H.; Farmer, D. L.; Harrison, M. R.; Keller, R. L.; Nobuhara, K. K. *J. Pediatric Surg.* **2006**, *41* (1), 29−33.
(21) Chang, E. I.; Galvez, M. G.; Glotzbach, J. P.; Hamou, C. D.; Elftesi, S.; Rappleye, C. T.; Sommer, K. M.; Rajadas, J.; Abilez, O. J.; Fuller, G. G.; Longaker, M. T.; Gurtner, G. C. *Nat. Med.* **2011**, *17* (9), 1147−U160.
(22) Hyman, N.; Manchester, T. L.; Osler, T.; Burns, B.; Cataldo, P. A. *Ann. Surg.* **2007**, *245* (2), 254−8.
(23) Chapman, W. C.; Clavien, P. A.; Fung, J.; Khanna, A.; Bonham, A. *Arch. Surg.* **2000**, *135* (10), 1200−4 discussion 1205..
(24) Abu Hilal, M.; Underwood, T.; Taylor, M. G.; Hamdan, K.; Elberm, H.; Pearce, N. W. *Surg. Endosc.* **2010**, *24* (3), 572−7.
(25) Wain, J. C.; Kaiser, L. R.; Johnstone, D. W.; Yang, S. C.; Wright, C. D.; Friedberg, J. S.; Feins, R. H.; Heitmiller, R. F.; Mathisen, D. J.; Selwyn, M. R. *Ann. Thoracic Surg.* **2001**, *71* (5), 1623−8 discussion 1628−9..
(26) Collet, J. P.; Park, D.; Lesty, C.; Soria, J.; Soria, C.; Montalescot, G.; Weisel, J. W. *Arterioscler Thromb. Vasc. Biol.* **2000**, *20* (5), 1354−61.
(27) Collet, J. P.; Shuman, H.; Ledger, R. E.; Lee, S.; Weisel, J. W. *Proc. Natl. Acad. Sci. U.S.A.* **2005**, *102* (26), 9133−7.
(28) Brown, X. Q.; Ookawa, K.; Wong, J. Y. *Biomaterials* **2005**, *26* (16), 3123−9.
(29) von Burkersroda, F.; Schedl, L.; Gopferich, A. *Biomaterials* **2002**, *23* (21), 4221−31.

(30) Lu, L.; Garcia, C. A.; Mikos, A. G. *J. Biomed. Mater. Res.* **1999**, *46* (2), 236–44.
(31) Ng, W. S.; Rosen, M. *Thorax* **1968**, *23* (2), 194–6.
(32) Moore, R. M.; Braselton, C. W. *Ann. Surg.* **1940**, *112* (2), 212–8.